



**Universiteit
Leiden**
The Netherlands

Structure, shape and dynamics of biological membranes.

Idema, T.

Citation

Idema, T. (2009, November 19). *Structure, shape and dynamics of biological membranes*. Retrieved from <https://hdl.handle.net/1887/14370>

Version: Corrected Publisher's Version

License: [Licence agreement concerning inclusion of doctoral thesis in the Institutional Repository of the University of Leiden](#)

Downloaded from: <https://hdl.handle.net/1887/14370>

Note: To cite this publication please use the final published version (if applicable).

CHAPTER 3

GIBBS PHASE DIAGRAMS OF TERNARY SYSTEMS

In this chapter we study the phase diagrams of ternary lipid mixtures. In particular we focus on the mixture of cholesterol, a saturated lipid and an unsaturated one. The phase diagram of such a lipid mixture exhibits a rich phase behavior with multiple phase coexistence regimes. Remarkably, phase separation even occurs when each of the three binary systems consisting of two of the three components is a uniform mixture. In the model we present here, we interpret the phase separation of the ternary system as a consequence of an interaction between all three components. For vanishing values of any of the three concentrations, the model reduces to the well-known Flory-Huggins model that describes the phase behavior of a binary system. From the associated Gibbs free energy we calculate phase diagrams, spinodals and critical points. Moreover, we use a Van der Waals / Cahn-Hilliard like construction to derive an expression for the line tension between coexisting phases. We show how the line tension depends on the position in the phase diagram, and give an explicit expression for the concentration profile at the phase boundary.

3.1 Introduction

Like any large collection of particles, lipids in a bilayer membrane have different levels of ordering dependent on thermodynamic parameters such as the temperature, and hence exhibit different phases. These phases are not only a function of thermodynamic variables such as the temperature, but also of the amount of ordering in the system. As introduced in section 1.2, the most common phases in which lipids can exist are a liquid-ordered (L_o), a liquid-disordered (L_d), and a gel phase. A membrane vesicle can have a uniform phase, but also exhibit coexistence of multiple phases, dependent on its lipid composition. In this chapter we introduce and review phase coexistence in lipid membranes with multiple components. We focus in particular on ternary membranes, which are the main subject of chapters 4, 5 and 6. In recent years, the phase diagrams of several ternary lipid systems have been determined experimentally [54, 55]. We use a simple extension of the Flory-Huggins model, which describes binary systems, to give a qualitative description of the different phase diagrams found in ternary lipid systems. Using the expression for the Gibbs free energy of this model, we can use a Van der Waals / Cahn-Hilliard like construction to derive an expression for the line tension between coexisting lipid phases as a function of membrane composition. This construction allows us to link experimental results on the phase diagrams to experimentally determined values of the line tension, and get new insights into how those two properties of the membrane are related to each other. Moreover, the line tension plays a critical role in the following chapters, as it is a key factor in determining the overall membrane shape.

3.1.1 Phase coexistence and the Gibbs phase triangle

In general, a phase diagram shows the conditions at which thermodynamically-distinct phases can occur at equilibrium, as a function of certain macroscopic variables like temperature, pressure, and composition. For a simple, one-component system, any point in a (p , T) phase diagram corresponds to a possible realization, and setting the pressure and temperature we obtain a uniform state for the entire system. Already for a bicomponent system this no longer needs to be the case, and apart from uniform phases we can also get coexistence of two distinct thermodynamic phases. The maximum number of phases P that can coexist in a given system is determined by the Gibbs phase rule [56, Chapter 9]

$$P = C - F + 2. \quad (3.1)$$

Here C is the number of components and F denotes the number of degrees of freedom, *i.e.*, the number of intensive variables which are independent of other intensive variables. For a two-component system in which temperature and pressure are the independent variables, two-phase coexistence is al-

lowed by equation (3.1). Figure 3.1 shows some schematic phase diagrams for a binary system as a function of the molar fraction x of one of the components and temperature, for a given pressure (please note that the complete phase diagrams are three-dimensional, with the pressure on the third axis, and the two-dimensional figures shown are slices through this complete diagram). Quenching the system below the phase boundary produces phase coexistence. For two thermodynamically different phases to coexist within one system, the values of the intrinsic variables must be equal. Here these are the temperature T , pressure p and the chemical potentials μ_A and μ_B of the two components A and B . Therefore the tie lines, which connect the two coexisting phases in the phase diagram, are in the plane of the figure (same pressure) and horizontal (same temperature) in figure 3.1.

The proper thermodynamic potential to use for describing this system is the Gibbs free energy \mathcal{G} , which has p , T and μ as its independent variables, and is given by

$$\mathcal{G} = E - TS + pV. \quad (3.2)$$

If we know \mathcal{G} for our binary system, we can find the phase boundary by the condition that the chemical potentials must be equal in the coexisting phases. They are given as derivatives of \mathcal{G} with respect to the number N_i of particles of type i (with $N_1 = xN$, $N_2 = (1-x)N$ and N the total number of particles in the system):

$$\mu_1 = \left(\frac{\partial \mathcal{G}}{\partial N_1} \right)_{p,T,N_2}, \quad \mu_2 = \left(\frac{\partial \mathcal{G}}{\partial N_2} \right)_{p,T,N_1}. \quad (3.3)$$

The Flory-Huggins model (section 3.1.2) gives a phenomenological expression for $\mathcal{G}(p, T, x)$ of a binary system which consists of a mixture of two polymers.

In the case of ternary systems, the Gibbs phase rule allows for coexistence of up to three different phases. Drawing the full phase diagram as a function of the two independent molar fractions, temperature and pressure would require four dimensions, limiting us to two- and three-dimensional slices. Two-dimensional slices for which both the temperature and pressure are given are known as Gibbs triangles. In these, each of the corners of the equilateral triangle corresponds to a system consisting solely of the associated component, the sides correspond to binary systems and the interior points to ternary systems. Because in an equilateral triangle the sum of the distances from any interior point to the three sides is equal, any point uniquely corresponds to a composition given by three molar fractions x , y and z , which sum to unity, see figure 3.2.

3.1.2 The Flory-Huggins model for a bicomponent system

Flory-Huggins theory is a mean-field, phenomenological model which describes the mixing properties of a system containing two types of polymers. Here we give a short sketch of the 2-component theory, where we assume that the

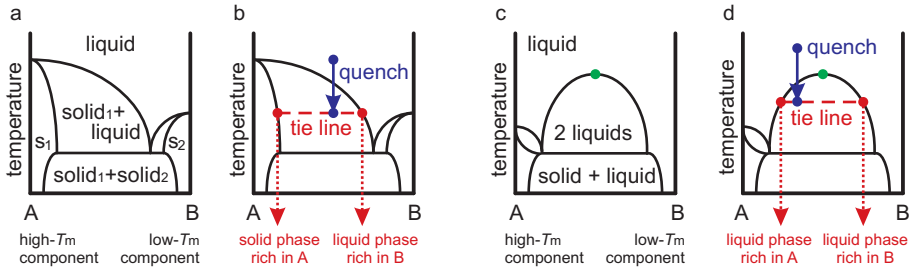


Figure 3.1: Schematic two-component phase diagrams, in terms of molar fraction x of component A and temperature T , for a given pressure. For high temperature, the system is in a uniform state. When we quench the system below the phase boundary (blue arrow) we obtain a system which exhibits coexistence of two thermodynamically different phases at the same temperature and pressure, but different compositions. The two coexisting phases are found at the intersections of the tie line with the phase boundary. Figures (a) and (b) show the situation in case we have coexistence of a solid and a liquid phase. Figures (c) and (d) show the coexistence of two liquid phases, which has a critical point (green dot).

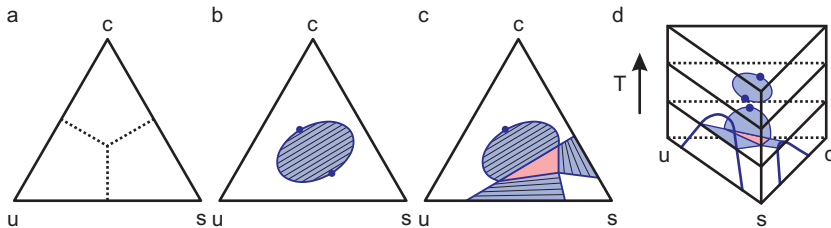


Figure 3.2: Gibbs phase triangle for a ternary system. The triangle represents a slice through the phase diagram at a given pressure and temperature. (a) The sum of the distances from any point in the equilateral triangle to the three edges equals 1. Every point in the Gibbs triangle corresponds to a composition of the ternary system with the concentrations corresponding to these distances to the edges. (b) Example of a phase diagram with a closed-loop miscibility gap. The two-phase coexistence region in the center has two critical points (blue dots). (c) Example of a phase diagram with multiple two-phase (blue) and a single three-phase (pink) coexistence regimes. (d) Possible Gibbs prism combining several Gibbs triangles.

monomers of the two species considered are equal in size. A more complete introduction can be found in many textbooks, *e.g.* Strobl [57, Chapter 3].

Suppose we prepare a system of polymers of type A and B such that the two are initially completely demixed and therefore effectively contained in separate volumes V_A and V_B . In the Flory-Huggins model, there are two contributions to the change in Gibbs free energy due to the mixing of this system. The first is an increase in entropy due to the larger total volume available to a single monomer of either type. The second contribution is due to individual monomer-monomer interactions. For uncharged monomers, the dominant interaction is Van der Waals attraction. Typically equal monomers will attract each other more strongly than unequal ones, in which case the second contribution to the free energy will oppose mixing.

The change in translational entropy is given by

$$\Delta\mathcal{S} = k_{\text{b}} \left[N_A \log \frac{N}{N_A} + N_B \log \frac{N}{N_B} \right] = -k_{\text{b}} N [x \log x + y \log y]. \quad (3.4)$$

Here $x = N_A/N$ and $y = N_B/N$ are the number fractions of species A and B respectively, $N = N_A + N_B$ is the total number of monomers, and k_{b} Boltzmann's constant. Because of the assumption that the monomers are equal in size, x and y are also the volume fractions of species A and B.

In a mean-field approach, the probability that a monomer of species A gets located next to one of species B is given by the product xy . We associate a free energy penalty $\chi k_{\text{b}} T$ to such a configuration and write for the monomer-monomer interaction contribution to the Gibbs free energy:

$$\Delta\mathcal{G}_{\text{loc}} = k_{\text{b}} T \chi N x y. \quad (3.5)$$

A negative value of the dimensionless Flory-Huggins parameter χ corresponds to an attractive interaction between monomers of species A and B and drives mixing, while a positive value of χ , which is the typical case, opposes it.

The total change in Gibbs free energy due to mixing is given by

$$\mathcal{G} = -T\Delta\mathcal{S} + \Delta\mathcal{G}_{\text{loc}} = k_{\text{b}} T N [x \log x + y \log y + \chi x y]. \quad (3.6)$$

Moreover, by construction, x and y add up to unity

$$x + y = 1, \quad (3.7)$$

which leaves us with a single-parameter minimization problem. In figure 3.3 we plot \mathcal{G} as a function of x for different values of χ .

From figure 3.3 it is clear that there are two possible scenarios. For small values of χ , \mathcal{G} has a single minimum and the system mixes for all values of x , the single freely adjustable parameter. For larger values of χ , \mathcal{G} has two minima, and although it can still be negative for all values of x , we do not get complete mixing in all cases. This is due to the fact that the system can reduce its Gibbs

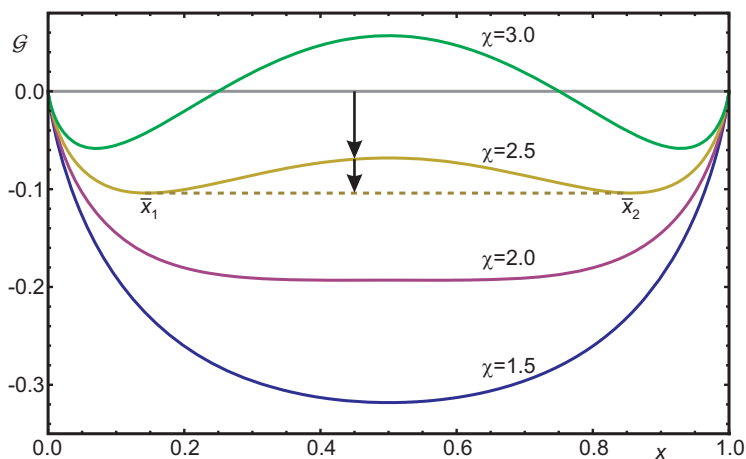


Figure 3.3: Change in Gibbs free energy due to mixing for various values of the Flory-Huggins parameter χ . For $\chi > \chi_{\text{crit}} = 2.0$, a miscibility gap opens: the free energy can be lowered by demixing, as illustrated by the two arrows for $\chi = 2.5$.

free energy with respect to the uniform mixture (corresponding to the local maximum) by segregating into two partially mixed fractions, corresponding to the two minima. This process is represented by the two arrows in figure 3.3 at $x = 0.45$ and $\chi = 2.5$. The long arrow, going down from $\mathcal{G} = 0$ to the graph of \mathcal{G} , represents the free energy gained by mixing the system. The short arrow going down from the graph to the line connecting the two minima, represents the additional free energy gain by segregating the system into domains with fractions \bar{x}_1 and \bar{x}_2 of species A. This process will occur for any initial value of x between \bar{x}_1 and \bar{x}_2 . This region is called the miscibility gap and its extremal values \bar{x}_1 and \bar{x}_2 are found by equating the chemical potentials (see section 3.2).

The critical value χ_c of the Flory-Huggins parameter, which determines whether or not the system mixes, is given by the point at which the curvature of \mathcal{G} vanishes at $x = 0.5$ (see section 3.2). A straightforward calculation shows that this condition holds for $\chi_c = 2$.

3.1.3 Ternary systems

In a ternary system, we have $C = 3$ and $F = 2$ (temperature and pressure) and hence the Gibbs phase rule (3.1) gives $P = 3$, so we can have up to three coexisting phases. In recent years several experimentally determined Gibbs phase triangles for ternary systems have been published, showing two- and three-phase coexistence regions [54]. As introduced in section 1.2, the three

phases that can coexist in ternary lipid membranes are two liquid phases (L_o and L_d) and a gel phase. Remarkably, there are also ternary systems for which each of the three limit binary systems is completely mixed, but for which the ternary system shows a two-phase coexistence region [55]. The boundary of the coexistence region in such a system is a closed loop inside the Gibbs phase triangle. Since phase coexistence is understood to be a consequence of what is known as a miscibility gap (as explained in section 3.1.2), such phase diagrams are said to contain a closed-loop miscibility gap.

A number of models for ternary lipid systems have been proposed by several groups in recent years. In a 2004 paper, Komura *et al.* [58] combined a Flory-Huggins like approach for liquid-liquid phase coexistence with an order parameter description for the liquid-gel phase transition and presented phase diagrams for two of the three limiting binary systems of the ternary system considered here. In a follow-up paper in 2005 [59] they extend this model to the ternary system, introducing three independent Flory-Huggins parameters for the three binary interactions and keeping the order parameter description for the gel phase. This model allows for a qualitative description of some of the experimentally observed phase diagrams, but fails to reproduce the one with the closed-loop miscibility gap. In an alternative approach, Radhakrishnan and McConnell [60] and McConnell [61] proposed a model in which two of the three components form a complex which interacts with the third component. The resulting phase diagram has some qualitative features which also appear in the closed-loop experimental one of Veatch *et al.* [55], but does not allow for three coexisting phases. Recently Putzel and Schick [62] presented a refined version of the model of Komura *et al.* They use two different models for the system with a closed-loop miscibility gap and the three-phase coexistence region, both depending on a combination of a Flory-Huggins model and an order-parameter description. Using these models, Putzel and Schick also studied the effect crosslinking molecules have on the phase diagram [63].

In section 3.3 we present a model for the ternary system based solely on an extension of the Flory-Huggins model of the binary system, and reducing to the binary models in each of the limit cases. In this model, we supplement the binary interactions with an interaction between all three components. This approach to model a ternary system is well known in the fields of alloys and of polymer mixtures [64–68], but thus far has not been applied to lipid mixtures. We show that the extension with a ternary term is necessary to explain the phase triangle with a closed-loop miscibility gap found experimentally by Veatch *et al.* [55] when the binary interactions are repulsive. The model can also reproduce the phase triangle with coexisting liquid and gel phases, as well as a three-phase coexistence region. We use our model to determine the linear stability of the system and explicitly find the critical points. Using the expression for the Gibbs free energy given by our model, we can calculate the energy associated with a boundary between two coexisting phases as a function of membrane composition (section 3.4). This boundary energy is a line ten-

sion in two-dimensional lipid membranes, and a key factor for determining the membrane shape [6, 10, 69–71].

3.2 Thermodynamics of mixtures

The appropriate characteristic function for describing phase equilibria in mixtures is the Gibbs free energy, which is a function of the particle numbers N_i , pressure p and temperature T

$$\mathcal{G} = \mathcal{G}(N_1, \dots, N_n, p, T). \quad (3.8)$$

The requirement for two phases to coexist is that all chemical potentials are equal in both phases, as well as the temperature and pressure (which is why \mathcal{G} is such a useful function for mixtures). The chemical potentials associated with each of the components are given by:

$$\mu_i = \frac{\partial \mathcal{G}}{\partial N_i}, \quad (3.9)$$

where the partial derivatives are taken with all the other variables constant. The total number of particles $N = N_1 + \dots + N_n$ is constant and taken as the extensive variable, and we define

$$\mathcal{G}/N = g(x_1, \dots, x_n) \quad \text{with} \quad x_i = N_i/N. \quad (3.10)$$

The number fractions x_i have a redundancy, and obey the condition

$$x_1 + \dots + x_n = 1, \quad (3.11)$$

which will allow us to eliminate one of them below. We can write the chemical potentials explicitly as functions of g and its derivatives to the x_i 's, showing that they are intensive

$$\mu_i = g + \frac{\partial g}{\partial x_i} - \sum_{j=1}^n x_j \frac{\partial g}{\partial x_j}. \quad (3.12)$$

These derivatives are unrestricted, in the sense that only the other particle numbers N_k are kept fixed, not *e.g.* the total particle number N . Summing all the μ_i 's, we find that we also have the relation

$$g = \sum_{i=1}^n x_i \mu_i. \quad (3.13)$$

Because our system is restricted to the subspace defined by equation (3.11), we can eliminate one of the number fractions (which we take to be x_n) from

the problem. Within this subspace, equation (3.12) reads

$$\mu_i = g + \frac{\partial g}{\partial x_i} - \sum_{j=1}^{n-1} x_j \frac{\partial g}{\partial x_j} \quad i = 1, \dots, n-1 \quad (3.14)$$

$$\mu_n = g - \sum_{j=1}^{n-1} x_j \frac{\partial g}{\partial x_j} \quad (3.15)$$

where g and its derivatives are now functions of x_1, \dots, x_{n-1} .

The formalism given above applies to a system with any number of components. For simplicity we will restrict ourselves to ternary systems below. We will indicate the concentrations of the three components by x , y and z instead of x_1 , x_2 and x_3 . In order to have phase coexistence the chemical potentials of all three components must be equal in both phases. In our ternary system we find that phases with number fractions (\bar{x}_1, \bar{y}_1) and (\bar{x}_2, \bar{y}_2) can coexist if

$$\begin{aligned} \mu_1(\bar{x}_1, \bar{y}_1) &= \mu_1(\bar{x}_2, \bar{y}_2), \\ \mu_2(\bar{x}_1, \bar{y}_1) &= \mu_2(\bar{x}_2, \bar{y}_2), \\ \mu_3(\bar{x}_1, \bar{y}_1) &= \mu_3(\bar{x}_2, \bar{y}_2). \end{aligned} \quad (3.16)$$

The system (3.16) gives us three equations for the four unknowns $(\bar{x}_1, \bar{y}_1, \bar{x}_2, \bar{y}_2)$, which means that in the Gibbs phase triangle there can be a coexistence region, in accordance with the Gibbs phase rule (3.1). The boundary of the phase coexistence regime (which consists of pairs of points that satisfy (3.16)) is called the binodal. The phase coexistence region is thus an open subset of the Gibbs phase triangle. Any point inside this region is connected to two points on the binodal by a tie line. A system prepared in a composition corresponding to such a point will demix into two phases corresponding to the two endpoints of the tie line it lies on. If the binodal forms a closed loop, the system has a closed-loop miscibility gap.

Using the identities (3.14, 3.15), we find that there is an equivalent system of conditions for phase coexistence given by

$$\begin{aligned} g_x(\bar{x}_1, \bar{y}_1) &= g_x(\bar{x}_2, \bar{y}_2), \\ g_y(\bar{x}_1, \bar{y}_1) &= g_y(\bar{x}_2, \bar{y}_2), \\ g(\bar{x}_1, \bar{y}_1) - \bar{x}_1 g_x(\bar{x}_1, \bar{y}_1) - \bar{y}_1 g_y(\bar{x}_1, \bar{y}_1) &= g(\bar{x}_2, \bar{y}_2) - \bar{x}_2 g_x(\bar{x}_2, \bar{y}_2) - \bar{y}_2 g_y(\bar{x}_2, \bar{y}_2), \end{aligned} \quad (3.17)$$

where subscripts x and y on $g(x, y)$ denote derivatives with respect to x and y . The first equation of (3.17) is found by subtracting μ_3 from μ_1 , the second by subtracting μ_3 from μ_2 and the third is identical to the third of (3.16).

The binodal separates the region in the phase diagrams in which our system is in a homogeneous phase from those in which it separates into two or three coexisting phases. However, in this simple Van der Waals type of phase

coexistence, the appearance of an unstable regime in the Gibbs phase triangle is a prerequisite. We therefore study the linear stability of our system at such a point (x, y) in a ternary system. We can vary both number fractions independently, and find for the variation in Gibbs free energy per particle

$$\delta g = \frac{1}{2}(\delta x, \delta y) \begin{pmatrix} g_{xx} & g_{xy} \\ g_{xy} & g_{yy} \end{pmatrix} \begin{pmatrix} \delta x \\ \delta y \end{pmatrix} + \mathcal{O}(3) \quad (3.18)$$

where $\mathcal{O}(3)$ refers to third order terms in δx and δy . For the second order term in (3.18) to vanish the determinant of the matrix (g_{ij}) of second order derivatives of g must be equal to zero. This condition also holds for systems with more than three components, and in general we find that the system becomes linearly unstable when

$$\det(g_{ij}) = 0. \quad (3.19)$$

We call the set of solutions of (3.19) the spinodal, because it marks the boundary between two types of demixing. Linearly stable systems demix by nucleation and growth and linearly unstable ones by spinodal decomposition [57, 72]. They are qualitatively different: in the case of nucleation and growth there is a nucleation barrier for the system to overcome before phase separation can take place, which is absent in the case of spinodal decomposition. Binary polymer systems, described by similar two-component Flory-Huggins models, also exhibit distinctly different patterning in the binodal (nucleated) and spinodal regimes [57, Chapter 3].

Equation (3.19) is equivalent with the condition that (g_{ij}) must have a zero eigenvalue, and if (3.19) holds the eigenvalue equation

$$\sum_{j=1}^2 g_{ij} r_j = 0, \quad (3.20)$$

has a solution in spinodal points. The eigenvector $\vec{r} = (r_1, r_2)$, belonging to the eigenvalue 0, is a direction in which all the thermodynamic potentials are stationary. To prove this statement, we consider a small displacement $(dx, dy) = (r_1, r_2)ds$ along \vec{r} from a point on the spinodal. Taking the derivative of the chemical potential μ_i along \vec{r} we find

$$\begin{aligned} \frac{\partial \mu_i}{\partial s} &= \frac{\partial \mu_i}{\partial x} \frac{\partial x}{\partial s} + \frac{\partial \mu_i}{\partial y} \frac{\partial y}{\partial s} \\ &= (g_{i1} - xg_{11} - yg_{21})r_1 + (g_{i2} - xg_{12} - yg_{22})r_2 \\ &= (g_{i1}r_1 + g_{i2}r_2) - (g_{11}r_1 + g_{12}r_2)x - (g_{21}r_1 + g_{22}r_2)y \\ &= 0 \end{aligned} \quad (3.21)$$

where the expressions in brackets in the third line of (3.21) all vanish because of (3.20). In general the direction (r_1, r_2) will intersect with the spinodal. In

special (critical) points the direction (r_1, r_2) will be tangent to the spinodal. There two neighboring points will have the same thermodynamic potentials according to (3.21) and are thus also coexisting. In the critical points the spinodal and binodal therefore touch, and the length of the tie lines goes to zero. Critical points are hence the limiting points of coexistence.

We can use equation (3.20) to find the critical points in a ternary system. We first note that equation (3.20) implies that the second derivative of g in the direction (r_1, r_2) vanishes:

$$\sum_{i,j=1}^2 g_{ij} r_i r_j = 0. \quad (3.22)$$

Equation (3.22) follows from (3.20) by multiplication with r_i and summing over i as well as j . In the critical point, where $\vec{r} = (r_1, r_2)$ is tangent to the spinodal, the determinant is stationary (remaining zero), so we have

$$\sum_{i,j,k=1}^2 g_{ijk} r_i r_j r_k = 0, \quad (3.23)$$

which means that the third derivative of g in the direction of \vec{r} vanishes. Combined, equations (3.22) and (3.23) give the conditions for a critical point.

A final question concerns the disappearance of the instability region from composition space. Then the derivative of the determinant will be zero in all directions. Equivalently, using equation (3.23) for the independent x and y directions, we have

$$g_{xxx} = g_{yyy} = 0. \quad (3.24)$$

Together with equation (3.19), equation (3.24) determines what we will call a ternary critical point, or the onset of phase separation. Such a ternary critical point usually does not occur in a Gibbs phase triangle, but if we add an additional axis (*e.g.* for temperature), the resulting three-dimensional phase prism will have such a point.

3.3 Model for ternary lipid mixtures

We denote the volume fractions of the saturated lipids, unsaturated lipids and cholesterol by x , y and z respectively. Analogously to the Flory-Huggins model, we take the fully demixed state as our reference state, and consider the change in Gibbs free energy due to mixing

$$\mathcal{G} = -T\Delta S + \Delta\mathcal{G}_{\text{loc}}. \quad (3.25)$$

The change in entropy by the increase in available volume when going from a demixed state to a mixed state is $-k_B N_i \log x_i$ for each of the three components (where \log indicates the natural logarithm, x_i as before the number fraction

of the i th component and N_i its total number of molecules). In our ternary system we have

$$\Delta S = -k_b N [x \log x + y \log y + z \log z]. \quad (3.26)$$

For each of the three binary mixtures we introduce a Flory-Huggins like local energy term. We assume that the volume is extensive, *i.e.*, scales linearly with the total number of particles N in the system, and therefore x_i is also the volume fraction of the i th component. The probability for two different molecules to encounter each other scales with both their volume fractions. The difference in interaction energy between two identical and two different nearest-neighbor molecules is given by the dimensionless parameter χ [57]. The local interaction term for a mixture of x and y is therefore given by $k_b TN \chi xy$. Below we will show that a model with just three binary interaction terms can not reproduce the experimentally observed phase diagrams. We therefore add another term, which depends on all three volume fractions [64, 68]. This addition supposes a significant contribution from a third-order term to the total free energy. There are two reasons why such a third-order term may occur. The first is if one of the components (here the cholesterol) acts as a line active agent for the phase separation of the other two [73, 74]. In that case all three need to come together at a single point in space, and hence a third-order term emerges. The second option is essentially the one suggested by Radhakrishnan and McConnell [60, 61], which is supported both by numerical studies [75–77] as well as some tentative experimental data [78, 79]. It supposes that the saturated lipids and the cholesterol form complexes, which subsequently interact with the unsaturated lipids. The difference between the model of Radhakrishnan and McConnell and the one proposed here, is that we simply look at the individual components, reflecting the fact that binary complexes are short-lived and continually form and dissociate, as is also seen in simulations [80]. A third order term emerges by combining the probabilities of a two-component complex to form and it meeting up with the third component.

Combining all contributions, we postulate for the local interaction term

$$\Delta \mathcal{G}_{\text{loc}} = k_b TN [\chi_{xy} xy + \chi_{xz} xz + \chi_{yz} yz + \bar{\chi} xyz], \quad (3.27)$$

and for the total change in Gibbs free energy we have

$$\frac{1}{N k_b T} \mathcal{G} = x \log x + y \log y + z \log z + \chi_{xy} xy + \chi_{xz} xz + \chi_{yz} yz + \bar{\chi} xyz, \quad (3.28)$$

with (as before, by definition)

$$x + y + z = 1. \quad (3.29)$$

Putting one of the three number fractions equal to zero in equation (3.28), we get the Flory-Huggins model for a binary system, as given by equation (3.6).

A straightforward calculation which can be found in many textbooks (see for example Strobl [57]), tells us that if the corresponding Flory-Huggins parameter χ is less than 2 the entropy term wins and the system is in a single homogeneous phase. If $\chi > 2$ a miscibility gap opens up and the free energy can be lowered by demixing into two coexisting phases.

The ternary term in (3.27) is the only ternary term we can add without changing the underlying binary systems, which is why we do not add any other ternary terms (*e.g.* an xy term). As we will show below, the ternary term is necessary to explain the existence of a closed loop miscibility gap in systems where the interactions between any pair of the three components are repulsive (*i.e.*, their χ parameters are positive). If there are attractive interactions instead (*e.g.* because one of the components is a solvent for one or both of the others), a closed loop miscibility gap can be described in a system with just the binary interactions [64]. In that case, the closed-loop immiscibility gap results from an asymmetry in the interaction parameters between the three pairs, which is called a $\Delta\chi$ -effect [66].

Substituting the free energy given by equation (3.28) in the equations of section 3.2, we can calculate Gibbs phase triangles for given values of χ_{xy} , χ_{xz} , χ_{yz} , and $\bar{\chi}$, and find the binodals, spinodals and critical points. If χ_{xy} , χ_{xz} and χ_{yz} are all less than 2, the corresponding binary systems are homogeneous, but for $\bar{\chi}$ above a critical value the ternary system can still exhibit phase coexistence. An example of a phase diagram with such a closed-loop miscibility gap is given in figure 3.4. The figure shows the binodal and tie lines, which we determine by numerically solving the system given by (3.16). It also shows the spinodal (the solution of equation (3.19)), which in the model given by (3.28) is an algebraic expression in x and y , and the two critical points. We find both the spinodal and the critical points by numerically solving their respective algebraic expressions.

Of course, we can also set the Flory-Huggins parameter of one of the binary mixtures above its critical value 2. If we do so with only one of them, we get a phase diagram with only one critical point, because the immiscibility region continues all the way to the edge of the Gibbs triangle (figure 3.7). In the case that two of the binary parameters allow for binary demixing, we can get more interesting phase diagrams. For certain combinations of the four parameters χ_{xy} , χ_{xz} , χ_{yz} and $\bar{\chi}$ there are three points in the phase triangle for which the chemical potentials match. These points are the vertices of a three-phase coexistence region. Inside there are no tie lines: any system corresponding to any of the points in the three-phase coexistence region will demix in the same fashion. The three-phase coexistence region is bordered by three two-phase coexistence regions, which we can identify as either liquid-liquid or liquid-gel by their densities. An example of such a phase diagram is shown in figure 3.5.

Finally, we use equations (3.19) and (3.24) to find the conditions for having a ternary critical point. Differentiating $g(x, y)$ three times, we find (reintroduc-

ing z to show the symmetry)

$$g_{xxx}(x, y) = \frac{1}{z^2} - \frac{1}{x^2} = 0, \quad (3.30)$$

$$g_{yyy}(x, y) = \frac{1}{z^2} - \frac{1}{y^2} = 0. \quad (3.31)$$

The system consisting of equations (3.29), (3.30) and (3.31) has a single solution: $x = y = z = 1/3$, which means that in our third-order theory a ternary critical point can only occur in the center of the Gibbs phase triangle. Substituting this point into equation (3.19), we find a condition on the parameters χ_{xy} , χ_{xz} , χ_{yz} and $\bar{\chi}$ for a ternary critical point to exist

$$27 - 6(\chi_{xy} + \chi_{xz} + \chi_{yz}) + 2(\chi_{xy}\chi_{xz} + \chi_{xy}\chi_{yz} + \chi_{xz}\chi_{yz}) - \chi_{xy}^2 - \chi_{xz}^2 - \chi_{yz}^2 \\ = \bar{\chi} \left(6 - \frac{2}{3}(\chi_{xy} + \chi_{xz} + \chi_{yz}) - \frac{1}{3}\bar{\chi} \right). \quad (3.32)$$

If we do not include the third order interaction term in (3.28), the right hand side of equation (3.32) vanishes. In that case there are no solutions for χ_{xy} , χ_{xz} and χ_{yz} all in the interval $[0, 2]$. Hence a ternary critical point can only exist if at least one of the underlying binary systems exhibits demixing (with $\chi > 2$) or has an attractive interaction between its components ($\chi < 0$). A system with repulsive interactions between all components can therefore only exhibit a closed loop miscibility gap if $\bar{\chi} > 0$. Given $\chi_{xy}(T)$, $\chi_{xz}(T)$ and $\chi_{yz}(T)$ from the underlying binary systems, equation (3.32) gives us the critical value of $\bar{\chi}$, or equivalently the critical temperature of our ternary system.

3.4 Phase boundary and line tension

Invoking Van der Waals / Cahn-Hilliard theory, we can use our explicit form of the free energy (3.28) to calculate the energy penalty for having a phase boundary. In our two-dimensional membrane system this boundary energy translates to a line tension between domains of different phases. For a detailed introduction into the scheme used here to derive an expression for the line tension, in particular equations (3.35) and (3.36) for a general Gibbs free energy, see Fisk and Widom [81].

We consider two coexisting liquid phases with compositions $(\bar{x}_1, \bar{y}_1, \bar{z}_1)$ and $(\bar{x}_2, \bar{y}_2, \bar{z}_2)$, where we eliminate z as usual. The concentrations do not make a jump at the domain boundary but rather have a smooth transition when we go from one domain to the other. We introduce a new variable s , which we use to parametrize the ‘position’ between the two phases: for $s \rightarrow -\infty$ we are in phase 1 and for $s \rightarrow \infty$ we are in phase 2. The origin $s = 0$ is determined as the

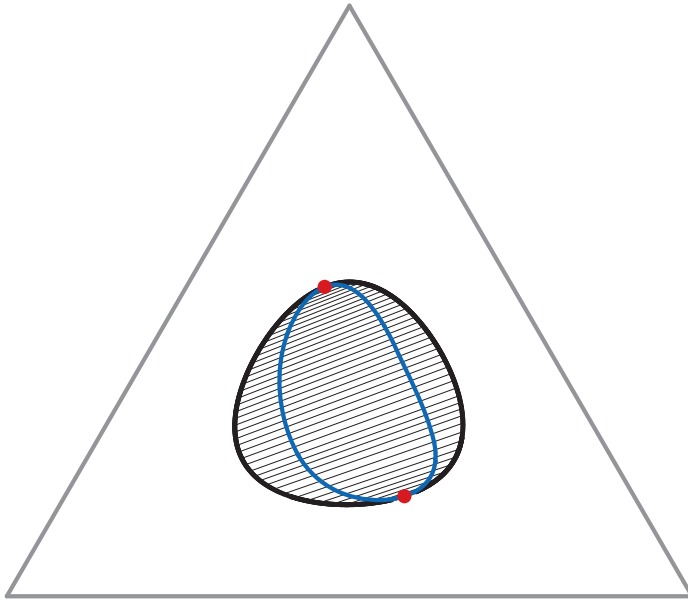


Figure 3.4: Gibbs phase triangle showing phase separation in the ternary system when there is none in any of the binary ones. The thick black line is the binodal, which marks the boundary of the immiscibility region. Any composition corresponding to a point inside the immiscibility region will result in demixing into two states, which are at the ends of the corresponding tie lines (thin black lines). The gray line inside the immiscibility region is the linear instability line (sometimes called the spinodal): points inside the region bordered by the gray line correspond to compositions that will demix by spinodal decomposition, points outside it will demix by nucleation and growth. The thick gray dots indicate the critical points. Parameters used: $\chi_{xy} = 1.5$, $\chi_{yz} = 1.25$, $\chi_{xz} = 0.75$, $\bar{\chi} = 5.0$.

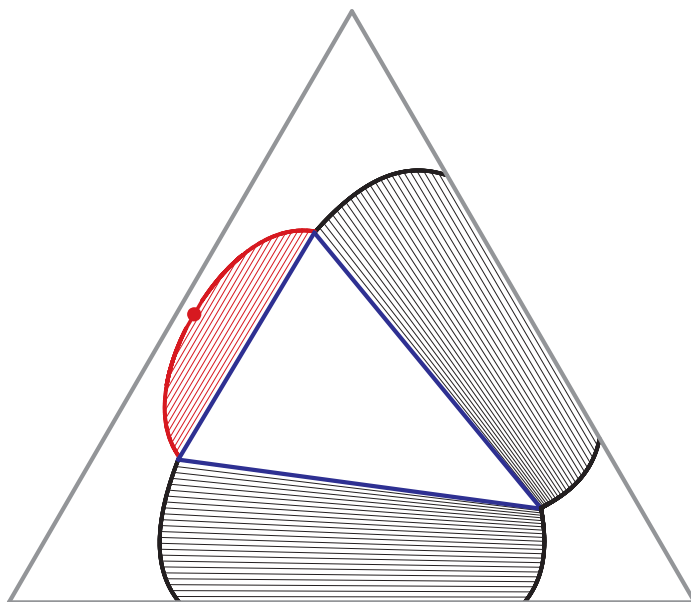


Figure 3.5: Gibbs phase triangle showing separation into two phases (the regions with the thin black and gray lines, which represent tie lines) and three phases (inside the black triangle; the compositions of the three phases correspond to the vertices of the triangle). The regions with black tie lines correspond to the coexistence of a gel and a liquid phase; the region with the gray tie lines corresponds to liquid-liquid coexistence, with a critical point indicated by the thick gray dot. The system is in a homogeneous gel phase in the lower right-hand region and in a homogeneous liquid phase in the left-hand region. Parameters used: $\chi_{xy} = 2.2$, $\chi_{xz} = 1.95$, $\chi_{yz} = 2.15$, $\bar{\chi} = 4.0$.

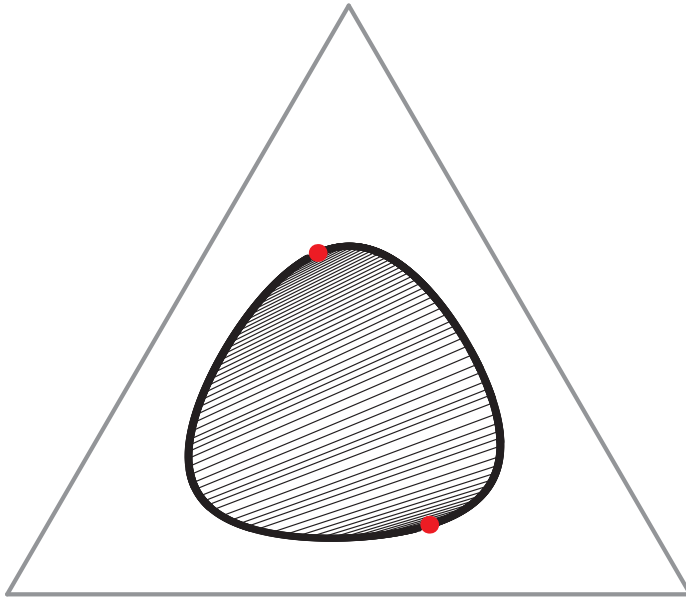


Figure 3.6: Gibbs phase triangle showing phase separation in the ternary system when there is none in any of the binary ones, but one of the binary interactions is attractive. The thick black line is the binodal, which marks the boundary of the immiscibility region. Any composition corresponding to a point inside the immiscibility region will result in demixing into two states, which are at the ends of the corresponding tie lines (thin black lines). The thick gray dots indicate the critical points. In this case, we find numerically that the coexistence region vanishes if the value of the ternary interaction parameter $\bar{\chi}$ is set to 0. Parameters used: $\chi_{xy} = 1.5$, $\chi_{yz} = 1.0$, $\chi_{xz} = -0.5$, $\bar{\chi} = 5.0$.

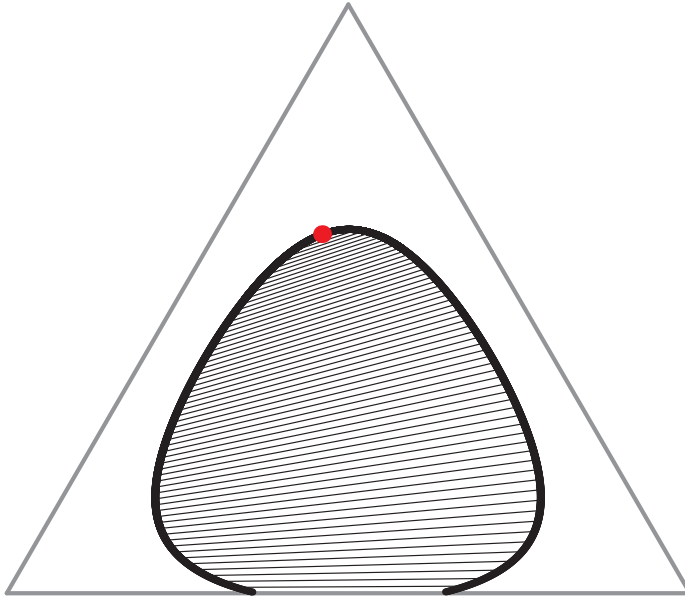


Figure 3.7: Gibbs phase triangle showing phase separation in the ternary system, when one of the underlying binary systems also exhibits phase separation. The thick black line is the binodal, which marks the boundary of the immiscibility region. Any composition corresponding to a point inside the immiscibility region will result in demixing into two states, which are at the ends of the corresponding tie lines (thin black lines). The thick gray dot indicates the critical point. Parameters used: $\chi_{xy} = 2.05$, $\chi_{yz} = 1.25$, $\chi_{xz} = 0.75$, $\bar{\chi} = 5.0$.

location of the Gibbs dividing surface

$$0 = \int_{-\infty}^0 \left[\lambda_x(x(s) - \bar{x}_1) + \lambda_y(y(s) - \bar{y}_1) \right] ds + \int_0^{\infty} \left[\lambda_x(x(s) - \bar{x}_2) + \lambda_y(y(s) - \bar{y}_2) \right] ds, \quad (3.33)$$

with λ_x and λ_y to be determined. The line tension is then given by the integral of the free energy density $\Psi(x, y)$ (to be defined below):

$$\tau = \int_{-\infty}^0 \left[\Psi(x(s), y(s)) - \Psi(\bar{x}_1, \bar{y}_1) \right] ds + \int_0^{\infty} \left[\Psi(x(s), y(s)) - \Psi(\bar{x}_2, \bar{y}_2) \right] ds. \quad (3.34)$$

The key assumption of the Van der Waals / Cahn-Hilliard theory is that Ψ exists for all values of s , and is given by the Gibbs free energy per particle $g(x, y)$ plus a quadratic gradient that accounts for the inhomogeneity in the transition region:

$$\Psi(x(s), y(s)) = g(x(s), y(s)) + \frac{A}{2} (\dot{x}^2 + \dot{y}^2), \quad (3.35)$$

where dots denote derivatives with respect to s . Here we make the simplifying assumption that the y -component of the 'kinetic energy' term has the same 'mass' A as the x -component. We can combine the expression for the line tension with the condition (3.33) into a single functional, where λ_x and λ_y play the role of Lagrange multipliers:

$$\tau = \int_{-\infty}^{\infty} \left[g(x(s), y(s)) - \bar{g}_{12} + \frac{A}{2} (\dot{x}^2 + \dot{y}^2) - \lambda_x(x(s) - \bar{x}_{12}) - \lambda_y(y(s) - \bar{y}_{12}) \right] ds, \quad (3.36)$$

where \bar{g}_{12} means $g(\bar{x}_1, \bar{y}_1)$ for $s \leq 0$ and $g(\bar{x}_2, \bar{y}_2)$ for $s \geq 0$ with corresponding definitions for \bar{x}_{12} and \bar{y}_{12} . Considering the integrand of (3.36) as a Lagrangian, we can invoke the Euler-Lagrange equations and find that for a stable interface ($\delta\tau = 0$) we must have

$$0 = A\ddot{x} - g_x(x(s), y(s)) + \lambda_x, \quad (3.37)$$

$$0 = A\ddot{y} - g_y(x(s), y(s)) + \lambda_y. \quad (3.38)$$

Because the derivatives of $x(s)$ and $y(s)$ must vanish for $s \rightarrow \pm\infty$, we find from equations (3.37) and (3.38) for the values of λ_x and λ_y :

$$\lambda_x = g_x(\bar{x}_1, \bar{y}_1) = g_x(\bar{x}_2, \bar{y}_2), \quad (3.39)$$

$$\lambda_y = g_y(\bar{x}_1, \bar{y}_1) = g_y(\bar{x}_2, \bar{y}_2). \quad (3.40)$$

Equations (3.39) and (3.40) are identical to the first and second condition of system (3.17) which determines the binodal. Equations (3.37) and (3.38) are the equations giving Newton's law of motion in the x and y direction of a particle with mass A that experiences a potential $V(x, y)$ given by

$$V(x, y) = -g(x, y) + \lambda_x x + \lambda_y y. \quad (3.41)$$

Moreover, since s does not explicitly appear in the Lagrangian, there is a conserved quantity. In mechanics, this property corresponds to translational invariance, and the conserved quantity is equivalent to the energy of the particle system:

$$E = \frac{A}{2}(\dot{x}^2 + \dot{y}^2) + V(x, y). \quad (3.42)$$

Again taking the limits $s \rightarrow \pm\infty$ we find for E :

$$\begin{aligned} E &= -g(\bar{x}_1, \bar{y}_1) + g_x(\bar{x}_1, \bar{y}_1)\bar{x}_1 + g_y(\bar{x}_1, \bar{y}_1)\bar{y}_1 \\ &= -g(\bar{x}_2, \bar{y}_2) + g_x(\bar{x}_2, \bar{y}_2)\bar{x}_2 + g_y(\bar{x}_2, \bar{y}_2)\bar{y}_2, \end{aligned} \quad (3.43)$$

which is identical to the third condition of (3.17).

So far we have expressed both $x(s)$ and $y(s)$ in s independently, but in order to find an expression of the line tension as an integral over the concentration x , we now express $y(s)$ in x , and write

$$E = \frac{A}{2}(1 + y'(x)^2)\dot{x}^2 + V(x, y(x)), \quad (3.44)$$

where the prime denotes a derivative with respect to x . Equation (3.44) gives us an expression for \dot{x} :

$$\dot{x} = \sqrt{\frac{2}{A} \frac{\sqrt{E - V(x, y(x))}}{\sqrt{1 + y'(x)^2}}}. \quad (3.45)$$

Using equations (3.41), (3.44) and (3.45) we can rewrite the expression for the line tension (3.36) as

$$\begin{aligned} \tau &= A \int_{-\infty}^{\infty} (1 + y'(x)^2)\dot{x}^2 ds \\ &= A \int_{\bar{x}_1}^{\bar{x}_2} (1 + y'(x)^2)\dot{x} dx \\ &= \sqrt{2A} \int_{\bar{x}_1}^{\bar{x}_2} \sqrt{1 + y'(x)^2} \sqrt{E - V(x, y(x))} dx \end{aligned} \quad (3.46)$$

Equation (3.46) again gives a functional expression for the line tension, for which we can again write down the Euler-Lagrange equations to get a differential equation for the optimal path $y(x)$. Because the integrand in (3.46) depends explicitly on x , there is no conserved quantity in this system. Performing

the variational analysis, we find after some algebra

$$y''(x) = \frac{1 + y'(x)^2}{2(E - V(x, y))} \left(-\frac{\partial V(x, y)}{\partial y} + \frac{\partial V(x, y)}{\partial x} y'(x) \right). \quad (3.47)$$

It seems straightforward to determine the optimal path from (\bar{x}_1, \bar{y}_1) to (\bar{x}_2, \bar{y}_2) by direct integration of the second-order differential equation (3.47). Unfortunately, there are two complications. The first is that both endpoints are singular points because $y''(x)$ tends to diverge close to the endpoints due to the factor $E - V(x, y(x))$ in the denominator of equation (3.47). The second complication is that the integration of the entire path is highly unstable. To avoid these complications we optimize τ by making a guess for $y(x)$, and compare the guess to equation (3.47). The most obvious guess is a straight line, *i.e.*, $y(x)$ follows the tie line that connects (\bar{x}_1, \bar{y}_1) with (\bar{x}_2, \bar{y}_2) , which gives us an upper bound for the value of τ . However, a better guess can be made by assuming a quadratic profile which has a free parameter that we can optimize (*i.e.*, tune it such that we find the lowest possible value of τ , or the ‘best’ solution of equation (3.47)). We notice that, according to this numerical approximation, the direction of $y(x)$ at the points at which it intersects the spinodal, coincides with that of the eigenvector \vec{r} associated with the zero eigenvalue of (g_{ij}) , (*i.e.*, the unstable direction, see figure 3.8). Although these quadratic profiles do not exactly solve equation (3.47), the deviation is small and only significant close to the endpoints. Because there the factor $\sqrt{E - V(x, y(x))}$ in the expression for τ vanishes, the estimate for τ using the quadratic profile is a reliable one. In appendix 3.A we show how to turn the first complication into an advantage, by which we can improve the guess, using a quartic profile. However, as we also show, the improvement of the estimate of τ using this quartic profile is negligible with respect to the optimal parabola.

3.5 Summary and discussion

In this chapter we have introduced phase diagrams of ternary mixtures. We have briefly reviewed the thermodynamics of mixtures, and the Flory-Huggins model which describes binary systems. Moreover, we have reviewed the models currently available in the literature to describe the phase diagrams at given temperature and pressure (Gibbs triangles) of ternary mixtures. None of these models succeed in capturing both the existence of a 3-phase coexistence region and (at different temperatures) a closed-loop miscibility gap. We have shown that using a simple extension of the Flory-Huggins model, namely the introduction of a third order interaction term, already well known in the fields of alloys and of polymer mixtures, is capable of capturing both effects in a single model. Moreover, we have shown that simply adding the three binary interactions without a third order term is insufficient to reproduce the closed-loop

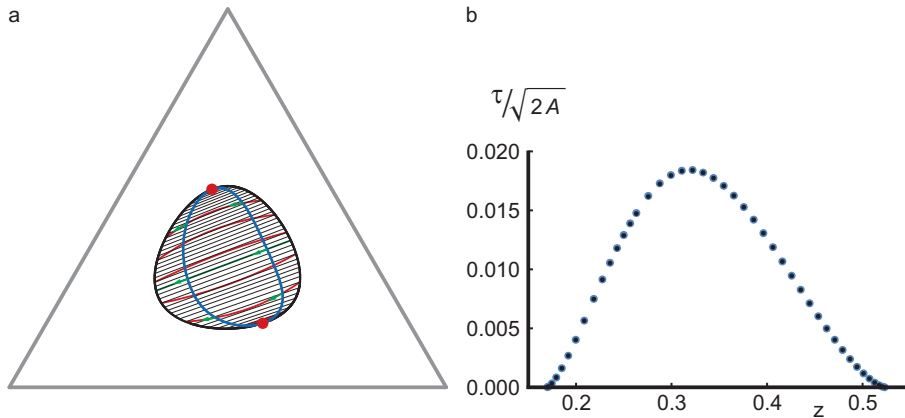


Figure 3.8: Line tension estimates using an optimized quadratic profile for $y(x)$ in equation (3.46). (a) Gibbs phase triangle showing the binodal (thick black line), tie lines (thin black lines), spinodal (blue line) and critical points (red dots). Some optimal quadratic paths connecting coexisting phases are shown (in red and green), as well as the directions of the eigenvectors of the zero eigenvalues of (g_{ij}) at the spinodal (in green). (b) Estimated values of $\tau/\sqrt{2A}$ determined using the optimal quadratic profiles shown in the left figure, as a function of 'position' between the critical points (the z -coordinate of the center of the corresponding tie line). The figure shows both the estimates determined using the optimal quadratic profiles shown in the left figure (big blue dots), as well as those determined using the optimal fourth-order profile as given in the appendix (small black dots); the positions of the points are indistinguishable in the plot. The line tension vanishes at both critical points and has a maximum when the optimal quadratic profile is a straight line, connecting the points on the binodal with the largest separation (green line in left figure). Parameters used: $\chi_{xy} = 1.5$, $\chi_{yz} = 1.25$, $\chi_{xz} = 0.75$, $\bar{\chi} = 5.0$.

miscibility gap if all binary interactions are repulsive, and even if one of them is weakly attractive.

Physically the ternary term we have added can be interpreted in at least two ways: the cholesterol may act as a line active agent at the phase boundary of the other two lipids, or alternatively, it may form a dynamic complex with one of the two other lipids which subsequently interacts with the remaining one. Since both the experimentally determined and the predicted tie-lines in the Gibbs triangles exhibiting liquid-liquid phase coexistence suggest that cholesterol is unequally distributed between the two liquid phases, we consider the second scenario to be the most probable one. However, in order to unambiguously distinguish between these two scenarios one should perform an experiment in which the cholesterol is labeled and its location determined in a (partially) phase separated lipid membrane vesicle.

In contrast to some of the other available models, the model we use does not take the effect of ordering into account. It is well known that the three different phases (L_d , L_o and gel) have different amounts of ordering, but it remains an open question whether this is a cause or a consequence of phase separation. We interpret the phase separation as the consequence of individual binary or ternary molecule-molecule interactions, but other approaches are certainly possible.

Using the ternary model given by equation (3.28) we have calculated the stability properties of the various phase diagrams, and determined the stability lines or spinodals, as well as the critical points. We have also derived an expression for the line tension between two coexisting phases in a lipid membrane system, as a function of the position in the phase diagram. This approach directly couples the line tension between coexisting domains, a key factor in the determination of the shape of lipid membrane vesicles, to the composition of the membrane.

Although the model we use qualitatively reproduces the experimentally observed features listed above, there is as yet no quantitative comparison to experiment. In principle such a comparison would be possible. The model for the Gibbs free energy has four free parameters, of which three are determined by the underlying binary systems and can be obtained from measurements on those. The fourth parameter ($\bar{\chi}$) can be determined experimentally using *e.g.* equation (3.32) for the ternary critical point. Given the values of these parameters, the value of the line tension can be calculated up to the overall proportionality factor A , which corresponds to a correlation length, and can in principle be determined independently. Experimental data with which this procedure can be carried out is currently not available. It might be possible to obtain such data with careful experiments, but they would be hard to carry out: the temperature, pressure and composition in all experimental systems should be controlled with high accuracy. Moreover, for each point in the phase diagram a new membrane has to be constructed, so the experiments would also be time-consuming. Apart from experimental difficulties, there is an impor-

tant assumption in this procedure which can not be checked directly, namely that the values of the binary interaction parameters remain unchanged in the ternary system. These parameters represent individual molecule-molecule interactions, for which we thus assume that the environment does not play an important role. Finally, in the derivation of the expression for the line tension τ , the expression for the free energy density Ψ given by (3.35) assumes that variations in the cholesterol concentration z are small, and that the scale factor A is identical for all lipids. Especially this last point is not necessarily true, and could affect estimates for τ using the calculations presented here.

In the next chapters, we will study the shape of (meta-)stable phase separated vesicles. The line tension on the boundaries will play an important role, both in the coarsening process (the merging of domains of the same phase) and in determining the shape. In chapter 4 we develop a model for the shape of a completely phase separated vesicle, based on the differential geometry techniques introduced in chapter 2, which we use to obtain the value of the line tension from experiments. In chapters 5 and 6 we study vesicles which are trapped in a kinetically arrested state. Their phase diagrams resemble the one given in figure 3.4. They are prepared at high temperature (such that their membrane is a uniform mixture), and subsequently quenched such that they end up in the liquid-liquid phase coexistence regime. They quickly nucleate domains, typically L_o domains in a L_d background. However, the domains do not all immediately merge, but remain stable for a long time, due to membrane deformations which are a result of the interplay between the line tension and the membrane's elastic bending energy. We study the patterns which emerge and sorting on the scale of the domains themselves.

3.A Optimal concentration profile

Close to the binodal, the factors $(E - V(x, y(x)))$, $\partial V(x, y)/\partial y$ and $\partial V(x, y)/\partial x$ in equation (3.47) all vanish. However, as we will show below, the first one vanishes quadratically with x , whereas the second and third only vanish linearly with x . Because the numerator and denominator of equation (3.47) should vanish equally fast as we approach the binodal in order for the second derivative of $y(x)$ to be well-defined, this allows us to find an expression for the first derivative of $y(x)$ at both ends of the interval. Those values we can use to improve our estimate of the concentration profile: since we now know both the endpoints and the derivatives at those endpoints, we have four set parameters and can optimize a fourth-order, instead of a quadratic, profile with a single optimization parameter. We will show that the fourth-order profile gives a marginal improvement in the estimate of the line tension τ , indicating that indeed the quadratic profile used in the main text gives a reliable estimate.

We rewrite equation (3.47) as an expression without fractions as

$$2(E - V(x, y))y''(x) = (1 + y'(x)^2) \left(-\frac{\partial V(x, y)}{\partial y} + \frac{\partial V(x, y)}{\partial x} y'(x) \right). \quad (3.48)$$

We reparametrize such that the origin is at the point around which we make our expansion (either (\bar{x}_1, \bar{y}_1) or (\bar{x}_2, \bar{y}_2)). We expand $y(x)$ around this origin and write

$$y(x) = a_1 x + a_2 x^2 + a_3 x^3 + a_4 x^4 + \dots \quad (3.49)$$

We also define

$$V_x = \frac{\partial V(x, y)}{\partial x}(0, 0) \quad (3.50)$$

$$V_y = \frac{\partial V(x, y)}{\partial y}(0, 0) \quad (3.51)$$

and likewise for higher-order derivatives. For the left-hand side of (3.48) we then find

$$2(E - V(x, y))y''(x) = a_2 (a_1^2 V_{yy} + 2a_1 V_{xy} + V_{xx}) x^2 + \mathcal{O}(x^3), \quad (3.52)$$

where we have left out all terms which are zero by virtue of equations (3.39), (3.40) and (3.43). The expansion of the right-hand side of (3.48) gives (again leaving out terms which are zero):

$$\begin{aligned} (1 + y'(x)^2) \left(-\frac{\partial V(x, y)}{\partial y} + \frac{\partial V(x, y)}{\partial x} y'(x) \right) = \\ - (1 + a_1^2) [(1 - a_1^2) V_{xy} + a_1 (V_{yy} - V_{xx})] x \\ + \frac{1}{2} \left[-2a_2 ((1 + 5a_1^2) V_{yy} + a_1 (1 - 7a_1^2) V_{xy} - 2(1 + 3a_1^2) V_{xx}) \right. \\ \left. + (1 + a_1^2) (-a_1^2 V_{yyy} - a_1 (2 - a_1^2) V_{xyy} \right. \\ \left. - (1 - 2a_1^2) V_{xxy} + a_1 V_{xxx}) \right] x^2 + \mathcal{O}(x^3). \quad (3.53) \end{aligned}$$

The lowest-order term of the left-hand side of equation (3.48) thus goes as x^2 , whereas the lowest-order term of the right-hand side goes as x . The coefficient of x should therefore vanish for equation (3.47) to be well-defined at the binodal, which gives the condition:

$$a_1^2 - \frac{V_{yy} - V_{xx}}{V_{xy}} a_1 - 1 = 0, \quad (3.54)$$

at both endpoints. Using condition (3.54) to calculate $y'(x)$ at \bar{x}_1 and \bar{x}_2 , we have four conditions on $y(x)$. We use those to fix four of the five parameters in a fourth-order polynomial approximation of $y(x)$, leaving a single parameter which we use to optimize τ in the same fashion as we did with the quadratic approximation. Figure 3.8 shows the values of τ we obtain from both the quadratic and fourth-order profiles, illustrating that they are virtually the same and showing that the quadratic approximation suffices.

